Energy-Efficient Wireless Powered Secure Transmission With Cooperative Jamming for Public Transportation

Linqing Gui, Bo He, Xiaobo Zhou, Chunhua Yu, Feng Shu, and Jun Li, *Senior Member, IEEE*

***Abstract*—In this paper, wireless power transfer and cooperative jamming (CJ) are combined to enhance physical security in public transportation networks. First, a new secure system model with both fixed and mobile jammers is proposed to guarantee secrecy in the worst-case scenario. All jammers are endowed with energy harvesting (EH) capability. Following this, two CJ-based schemes, namely, beamforming-CJ-SR-maximization (B-CJ-SRM) and beamforming-CJ-transmit-power-minimization (B-CJ-TPM), are proposed, where SRM and TPM are short for secrecy rate maximization and transmit power minimization, respectively. They, respectively, maximize the secrecy rate (SR) with transmit power constraint and minimize the transmit power of the BS with SR constraint, by optimizing beamforming vector and artificial noise covariance matrix. To further reduce the complexity of our proposed optimal schemes, their low-complexity (LC) versions, called LC-B-CJ-SRM and LC-B-CJ-TPM are developed. Simulation results show that our proposed schemes, B-CJ-SRM and B-CJ-TPM, achieve significant SR performance improvement over existing zero-forcing and QoSD methods. Additionally, the SR performance of the proposed LC schemes is close to those of their original versions.**

***Index Terms*—Energy harvesting, physical layer security, secrecy rate maximization, transmit power minimization.**

I. Introduction

FOR THE sake of green communication, wireless devices are urged to transmit with a very low power [1]. Meanwhile, due to broadcast nature, wireless signal is still vulnerable to eavesdroppers. Consequently, energy-efficient secure wireless communication has arisen to be an important issue [2]. So this paper focuses on energy-efficient secure communication issue in public places, especially in city public transportation vehicles. For example, when someone takes a city bus or light rail for one-hour business trip, he would utilize wireless networks to fulfill commercial tasks such as e-transaction and classified file transfer. If a commercial spy/eavesdropper who is disguised as a passenger in the same carriage, he can easily capture those sensitive information. Therefore, when potential eavesdroppers are detected, security techniques should be employed immediately to protect information transmission.

To address this issue, researchers have proposed encryption techniques as well as physical-layer (PHY) security techniques. As an effective supplement to encryption techniques, PHY security exploits the characteristics of wireless channels. One important criterion of PHY security is achievable secrecy rate (SR) defined as the difference between the transmission rate of the legitimate channel and that of the wiretap channel [3]. When the wiretap channel is worse than legitimate channel, the SR is easily downgraded below zero and secure transmission cannot be guaranteed. In order to improve the secrecy, many effective schemes have been proposed such as artificial noise (AN) [2], [4], directional modulation (DM) [5], [6] and cooperative jamming (CJ) [7]–[9]. AN is often generated by transmission node with multiple antennas to only degrade the wiretap channel. DM synthesis is achieved by transmitting confidential messages directly towards the desired receivers [5]. However, DM alone cannot solve security issue in public vehicle because Base Station (BS) can hardly generate beams that are narrow enough to directionally distinguish mobile nodes in the same carriage of a public vehicle.

On the contrary, CJ is preferable in public transportation because mobile devices carried by passengers are potentially helpful cooperative nodes which generate and transmit AN signals to interfere with the eavesdropper. Although CJ can enhance the SR, the performance is achieved at the cost of energy consumption of cooperative nodes. Since cooperative nodes, e.g., mobile devices are usually energy-starving, it is critical to fully compensate them through energy harvesting techniques [10], [11]. Radio frequency energy harvesting methods are normally separated into two types: simultaneous wireless information and power transfer (SWIPT) and wireless powered tranfer (WPT) [12]. In SWIPT, transmitted signals carry both energy and information to simultaneously achieve information delivery and energy recharging [13]. In contrast, WPT first recharges wireless nodes which then transmit

Manuscript received May 1, 2018; revised October 9, 2018, February 27, 2019, and June 7, 2019; accepted July 11, 2019. Date of publication July 22, 2019; date of current version November 20, 2019. This work was supported in part by the National Natural Science Foundation of China under Grant 61602245, Grant 61771244, Grant 61501238, Grant 61702258, Grant 61872184, and Grant 61727802, in part by the National Key Research and Development Program under Grant 2018YFB1004800, and in part by the Natural Science Research Project of Education Department of Anhui Province of China under Grant KJ2019A1002. The associate editor coordinating the review of this paper and approving it for publication was V. Mancuso. *(Corresponding author: Feng Shu.)*

L. Gui, B. He, X. Zhou, F. Shu, and J. Li are with the Department of Electronic and Optical Engineering, Nanjing University of Science and Technology, Nanjing 210094, China (e-mail: guilinqing@163.com; 1264722064@qq.com; zxb@njust.edu.cn; shufeng0101@163.com; jun.li@njust.edu.cn).

C. Yu is with the School of Electronic Science and Engineering, Nanjing University, Nanjing 210000, China (e-mail: yuch@nju.edu.cn).

Digital Object Identifier 10.1109/TGCN.2019.2930072

information by utilizing the harvested energy. WPT is more suitable than SWIPT in this paper because cooperative nodes only need the energy from power station.

Although either CJ or WPT has been well studied in literature, it is in recent years that their combination has become an attractive research topic [14]–[17]. In [14], a hybrid base station (BS) first transfers power to the source and then performs CJ while the source transmits information using the harvested energy. In the wireless-powered network described in [15], cooperative nodes helps to relay information from the source and some of them are assumed to be untrusted. The secure network in [16] comprises of one source, one jammer and one destination. The SR at the destination is maximized by jointly optimizing the power allocation at the source and the jammer as well as the time allocation between two time slots. In [17], CJ strategies for wireless powered communication networks are investigated. Designed for other scenarios, those strategies cannot be directly employed in public transportation. Focusing on PHY security issue in public transportation, the main contributions of this paper are summarized as follows.

(1) A CJ-based secure communication model with energy harvesting capability is established for public transportation. In this model CJ is fulfilled by both fixed and mobile jammers. The fixed jammers can help to guarantee basic secrecy performance in the worst case with no mobile users in the vehicle. If mobile users exist, they can act as mobile jammers to interfere with the eavesdropper. Energy harvesting is provided for mobile jammers to compensate their energy consumption.

(2) Beamforming-CJ-SR-maximization (B-CJ-SRM) and beamforming-CJ-transmit-power-minimization (B-CJ-TPM) are proposed to obtain the maximum secrecy and the minimum power, respectively. As to the two proposed schemes, original optimization problem is converted into a tractable semi-definite programming (SDP) problem by semi-definite relaxation (SDR). Simulation results show that the proposed schemes have better performance than some existing schemes such as zero-forcing [8] and QoSD [18].

(3) To reduce the complexity of the proposed optimal schemes, two low-complexity schemes are then designed. These two schemes namely LC-B-CJ-SRM and LC-B-CJ-TPM both employ concave convex procedure (CCCP) iterative method to obtain sub-optimal solutions. The complexity of the two schemes are proved to be much lower than that of the former optimal schemes. Simulation results show that they can also achieve similar performance to the optimal schemes.

The rest of this paper is organized as follows. Section II presents the CJ-based secure communication model. Section III describes our proposed two CJ-based optimal schemes. Section IV illustrates the low-complexity schemes. Simulation results in Section V validate the effectiveness and advantage of the proposed schemes. Section VI concludes the paper.

Notations: The lower-case, boldface lower-case and boldface upper-case letters are used to denote scalars, vectors and matrices, respectively. The transpose, conjugate, conjugate transpose, rank and trace of the matrix X are denoted as X^T, X^*, X^H, rank(X) and Tr(X), respectively. $X \succeq 0$ denotes that X is Hermitian positive semidefinite matrix. $E\{\cdot\}$ denotes expectation. $\log\{\cdot\}$ denotes the base-2 logarithm.

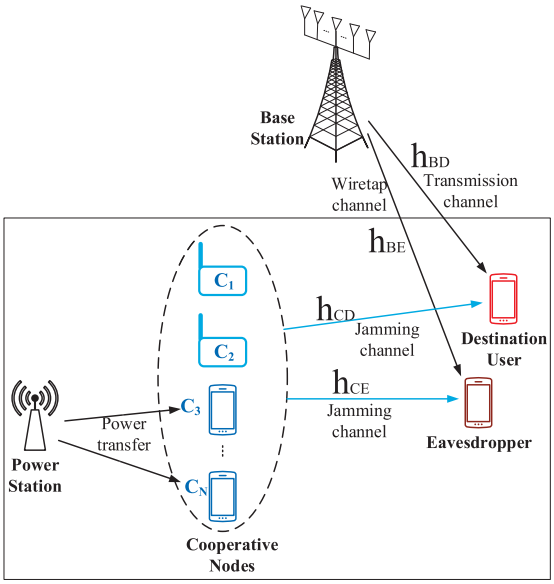

Fig. 1. System model.

II. System Model

As shown in Fig. 1, we consider a downlink secure communication system with one BS equipped with M antennas, one destination user, one eavesdropper, one power station and N cooperative nodes. Except the BS, all other nodes are deployed in a public vehicle and each has a single antenna. The destination user is actually a mobile user in the vehicle. Harvesting energy from the power station, cooperative nodes $C_1, C_2, C_3, \ldots, C_N$ are used to transmit jamming signals to deliberately confuse the eavesdropper. The first two cooperative nodes are fixed while the others are mobile jamming nodes which are actually mobile users. The two fixed nodes are used to guarantee a basic secrecy in the worst case of no mobile jamming nodes in the vehicle, probably in non-peak hours. In this case, the fixed jammers can still create some interference at the eavesdropper. At least two single-antenna fixed nodes are required to create different amounts of interference at the eavesdropper and destination user.

The mobile users in the vehicle are excellent jammers because some of them can locate close to the eavesdropper. In peak hours, a number of mobile users in the same vehicle can greatly interfere with the eavesdropper. To compensate the energy consumption of these helpers, a power station is used to transfer power to them. The transmit power of each cooperative node is limited to be less than its harvested power.

The information signal vector transmitted from the BS and the jamming signal vector transmitted from cooperative nodes are denoted by $\mathbf{v}x \in \mathbb{C}^{M\times 1}$ and $\mathbf{z} \in \mathbb{C}^{N\times 1}$ respectively, where $\mathbf{v}$ is beamforming vector, x is confidential information signal with $\mathbb{E}[x^H x] = 1$. Then the received signals at the destination user and the eavesdropper can be respectively

expressed as

$$y_d = \mathbf{h}_{BD}^H \mathbf{v}x + \mathbf{h}_{CD}^H \mathbf{z} + n_d, \tag{1}$$

$$y_e = \mathbf{h}_{BE}^H \mathbf{v}x + \mathbf{h}_{CE}^H \mathbf{z} + n_e, \tag{2}$$

where $\mathbf{h_{BD}} \in \mathbb{C}^{M\times 1}$ and $\mathbf{h_{BE}} \in \mathbb{C}^{M\times 1}$ respectively denote the transmission channel and wiretap channel, $\mathbf{h_{CD}} \in \mathbb{C}^{N\times 1}$ and $\mathbf{h_{CE}} \in \mathbb{C}^{N\times 1}$ respectively denote jamming channels from cooperative nodes to the destination user and the eavesdropper. All the channels are assumed to be available. Since the speed of public vehicles such as buses is usually less than 50km/h, Doppler shift is so small that the channels between the BS and in-vehicle mobile users can be accurately estimated [19].

The assumption that the eavesdropper's CSI (channel state information) is available can be justified by the fact that the eavesdropper can be a potential legitimate user which cooperates with the BS to conduct channel estimation. The channel state between the eavesdropper and cooperative nodes can be measured by D2D communication. When the eavesdropper transmits a sounding reference signal (SRS) over a common uplink channel, cooperative nodes can estimate its channels to the eavesdropper based on the received SRS signal [20].

In (1) and (2), n_d and n_e represent the additive white Gaussian noise with variance σ^2, at the destination and eavesdropper, respectively, while $\mathbf{z}$ is the zero-mean Gaussian AN vector. Let the diagonal matrix $\mathbf{Q} = \mathbb{E}[\mathbf{z}\mathbf{z}^H]$, $\mathbf{Q} \succeq 0$. If the maximum transmit power of the BS is P_{BS}, then we have

$$\mathbb{E}(|\mathbf{v}x|^2) = \mathbf{v}^2 \leq P_{BS}. \tag{3}$$

The transmit power of each cooperative node is set below a preset value or the harvested power, i.e.,

$$\mathbf{e}_i^T \mathbf{Q} \mathbf{e}_i \leq P_i, \quad i = 1, 2, \ldots, N, \tag{4}$$

where P_i ($i > 2$) is the harvested power of *i*-th cooperative node, while $\mathbf{e}_i$ is a column vector in which the *i*-th element is 1 and all other elements are all 0's. Following (1) and (2), the achievable rates from the BS to the destination and the eavesdropper are respectively given by

$$R_d = \log\left(1 + \frac{\left|\mathbf{h}_{BD}{}^H \mathbf{v}\right|^2}{\mathbf{h}_{CD}{}^H \mathbf{Q} \mathbf{h}_{CD} + \sigma^2}\right), \tag{5}$$

$$R_e = \log\left(1 + \frac{\left|\mathbf{h}_{BE}{}^H \mathbf{v}\right|^2}{\mathbf{h}_{CE}{}^H \mathbf{Q} \mathbf{h}_{CE} + \sigma^2}\right). \tag{6}$$

Then the achievable SR is $R_s = \max\{0, R_d - R_e\}$. In this work, a positive SR can be guaranteed due to the known CSI in our system model. So the achievable SR can be written as

$$R_s(\mathbf{v}, \mathbf{Q}) = R_d - R_e. \tag{7}$$

With the power constraints (3) and (4), our goal is to maximize $R_s(\mathbf{v}, \mathbf{Q})$ or to minimize BS transmit power with a certain level of SR. The goal is achieved in the following section through the optimization of $\mathbf{v}$ and $\mathbf{Q}$.

III. Proposed Joint Design of Secure Beamforming and Cooperative Jamming

In this section, we joint design the beamforming vector $\mathbf{v}$ and the covariance matrix $\mathbf{Q}$ to achieve the goal. Firstly B-CJ-SRM scheme is proposed to maximize $R_s(\mathbf{v}, \mathbf{Q})$, then B-CJ-TPM scheme is proposed to minimize the transmit power of the BS while guaranteeing $R_s(\mathbf{v}, \mathbf{Q}) \geq R_s^0$ where R_s^0 is the minimum required SR.

A. Proposed B-CJ-SRM

Originally, our objective is to maximize $R_s(\mathbf{v}, \mathbf{Q})$ subject to the power constraints (3) and (4). However, as per (7) we can see that maximizing R_s is to maximize a product of two correlated and generalized eigenvectors, which is difficult to solve. Although a linear search method can be used to solve this kind of problem [21], the computation is too complex. A less complex solution is feasible if there is a requirement on the eavesdropper's maximum SINR. To achieve a certain level of secrecy, it is rational to demand the eavesdropper's SINR stay below γ_e. Then a tractable solution can be achieved by reforming the maximization of $R_s(\mathbf{v}, \mathbf{Q})$ into that of the destination's SINR. So the optimization problem is given by

$$\begin{aligned} \max_{\mathbf{v},\mathbf{Q}} \ & \frac{\left|\mathbf{h}_{BD}^H \mathbf{v}\right|^2}{\mathbf{h}_{CD}^H \mathbf{Q} \mathbf{h}_{CD} + \sigma^2} \\ \text{s.t.} \ & |\mathbf{v}|^2 \leq P_{BS}, \\ & \mathbf{e}_i^T \mathbf{Q} \mathbf{e}_i \leq P_i, \quad i = 1, 2, \ldots, N, \\ & \frac{\left|\mathbf{h}_{BE}^H \mathbf{v}\right|^2}{\mathbf{h}_{CE}^H \mathbf{Q} \mathbf{h}_{CE} + \sigma^2} \leq \gamma_e, \\ & \mathbf{Q} \succeq \mathbf{0}. \end{aligned} \tag{8}$$

Let $\mathbf{V} = \mathbf{v}\mathbf{v}^H$, (8) can be rewritten as

$$\begin{aligned} \max_{\mathbf{v},\mathbf{V},\mathbf{Q}} \ & \frac{\mathbf{h}_{BD}^H \mathbf{V} \mathbf{h}_{BD}}{\mathbf{h}_{CD}^H \mathbf{Q} \mathbf{h}_{CD} + \sigma^2} \\ \text{s.t.} \ & \mathrm{Tr}(\mathbf{V}) \leq P_{BS}, \\ & \mathbf{e}_i^T \mathbf{Q} \mathbf{e}_i \leq P_i, \quad i = 1, 2, \ldots, N, \\ & \frac{\mathbf{h}_{BE}^H \mathbf{V} \mathbf{h}_{BE}}{\mathbf{h}_{CE}^H \mathbf{Q} \mathbf{h}_{CE} + \sigma^2} \leq \gamma_e, \\ & \mathbf{V} \succeq \mathbf{0}, \mathbf{Q} \succeq \mathbf{0}, \\ & \mathbf{V} = \mathbf{v}\mathbf{v}^H. \end{aligned} \tag{9}$$

Since $\mathbf{V} = \mathbf{v}\mathbf{v}^H$ is a non-convex constraint, if we remove it, (9) is converted to

$$\begin{aligned} \max_{\mathbf{V},\mathbf{Q}} \ & \frac{\mathbf{h}_{BD}^H \mathbf{V} \mathbf{h}_{BD}}{\mathbf{h}_{CD}^H \mathbf{Q} \mathbf{h}_{CD} + \sigma^2} \\ \text{s.t.} \ & \mathrm{Tr}(\mathbf{V}) \leq P_{BS}, \\ & \mathbf{e}_i^T \mathbf{Q} \mathbf{e}_i \leq P_i, \quad i = 1, 2, \ldots, N \\ & \mathbf{h}_{BE}^H \mathbf{V} \mathbf{h}_{BE} - \gamma_e \left(\mathbf{h}_{CE}^H \mathbf{Q} \mathbf{h}_{CE} + \sigma^2\right) \leq 0, \\ & \mathbf{V} \succeq \mathbf{0}, \mathbf{Q} \succeq \mathbf{0}. \end{aligned} \tag{10}$$

Although the objective function in (10) is quasi-convex, it can be converted to a convex one by Charnes-Cooper transformation [22]. Thus (10) can be rewritten as

$$\begin{aligned}\max_{\tilde{\mathbf{V}},\tilde{\mathbf{Q}},t}\ & \mathrm{Tr}\Big(\mathbf{H}_{BD}\tilde{\mathbf{V}}\Big)\\ \text{s.t.}\ & \mathrm{Tr}\Big(\tilde{\mathbf{V}}\Big) \le tP_{BS},\\ & \mathrm{Tr}\Big(\mathbf{e}_i\mathbf{e}_i^T\tilde{\mathbf{Q}}\Big) \le tP_i, i=1,2,\ldots,N,\\ & \mathrm{Tr}\Big(\mathbf{H}_{BE}\tilde{\mathbf{V}}\Big) - \gamma_e\Big(\mathrm{Tr}(\mathbf{H}_{CE}\tilde{\mathbf{Q}}) + \sigma^2 t\Big) \le 0,\\ & \mathrm{Tr}\Big(\mathbf{H}_{CD}\tilde{\mathbf{Q}}\Big) + \sigma^2 t = 1,\\ & \tilde{\mathbf{V}} \succeq \mathbf{0},\quad \tilde{\mathbf{Q}} \succeq \mathbf{0}, \end{aligned} \tag{11}$$

where t is a slack variable [23], [24], $\tilde{\mathbf{V}} = t\mathbf{V}$, $\tilde{\mathbf{Q}} = t\mathbf{Q}$, $\mathbf{H}_{BD} = \mathbf{h}_{BD}\mathbf{h}_{BD}^H$, $\mathbf{H}_{CD} = \mathbf{h}_{CD}\mathbf{h}_{CD}^H$, $\mathbf{H}_{BE} = \mathbf{h}_{BE}\mathbf{h}_{BE}^H$ and $\mathbf{H}_{CE} = \mathbf{h}_{CE}\mathbf{h}_{CE}^H$.

Since (11) is a standard SDP problem, its optimal solution $(\tilde{\mathbf{V}}^*, \tilde{\mathbf{Q}}^*, t^*)$ can be found by using CVX tools. Then the optimal solution of (10) is ($\mathbf{V}^* = \tilde{\mathbf{V}}^*/t^*$, $\mathbf{Q}^* = \tilde{\mathbf{Q}}^*/t^*$). If rank($\mathbf{V}^*$) is 1, $\mathbf{V}^*$ can be written as $\mathbf{V}^* = \mathbf{v}^*\mathbf{v}^{*H}$ based on eigenvalue decomposition. So (8) is solved and its optimal solution is $(\mathbf{v}^*, \mathbf{Q}^*)$. Since the constraint $\mathbf{V} = \mathbf{v}\mathbf{v}^H$ is removed when converting (9) into (10), we now only have to prove $\mathrm{rank}(\mathbf{V}^*) \le 1$ because $\mathrm{rank}(\mathbf{V}^*) \le 1$ is equivalent to $\mathbf{V} = \mathbf{v}\mathbf{v}^H$. This proof is detailed in the Appendix.

B. Proposed B-CJ-TPM

In previous subsection, to obtain the optimal SR, the BS will always transmit in its maximum power P_{BS}. Reducing the transmit power of the BS has considerable importance to green communication, because the BS usually transmits in a much higher power than in-vehicle nodes. To minimize the transmit power of the BS, the optimization problem is re-designed in this subsection with a new objective function and a SR constraint on its minimum value R_s^0. So the problem of transmit power minimization can be formulated as

$$\begin{aligned}\min_{\mathbf{v},\mathbf{Q}}\ & |\mathbf{v}|^2\\ \text{s.t.}\ & R_s(\mathbf{v},\mathbf{Q}) \ge R_s^0\\ & \mathbf{e}_i^T\mathbf{Q}\mathbf{e}_i \le P_i, i=1,2,\ldots,N\\ & \mathbf{Q} \succeq \mathbf{0}. \end{aligned} \tag{12}$$

Similar to the objective function in (8), the SR constraint in (12) is replaced with the limitation on the destination's SINR and the eavesdropper's SINR. Then (12) can be rewritten as

$$\begin{aligned}\min_{\mathbf{v},\mathbf{Q}}\ & |\mathbf{v}|^2\\ \text{s.t.}\ & \frac{\left|\mathbf{h}_{BD}^H\mathbf{v}\right|^2}{\mathbf{h}_{CD}^H\mathbf{Q}\mathbf{h}_{CD}+\sigma^2} \ge \gamma_d\\ & \frac{\left|\mathbf{h}_{BE}^H\mathbf{v}\right|^2}{\mathbf{h}_{CE}^H\mathbf{Q}\mathbf{h}_{CE}+\sigma^2} \le \gamma_e\\ & \mathbf{e}_i^T\mathbf{Q}\mathbf{e}_i \le P_i, i=1,2,\ldots,N\\ & \mathbf{Q} \succeq \mathbf{0}, \end{aligned} \tag{13}$$

where $R_s^0 = \log(1+\gamma_d) - \log(1+\gamma_e)$, so γ_d can be expressed as a function of R_s^0 and γ_e. Let $\mathbf{V} = \mathbf{v}\mathbf{v}^H$, (13) is converted to

$$\begin{aligned}\min_{\mathbf{v},\mathbf{V},\mathbf{Q}}\ & \mathrm{Tr}(\mathbf{V})\\ \text{s.t.}\ & \frac{\mathbf{h}_{BD}^H\mathbf{V}\mathbf{h}_{BD}}{\mathbf{h}_{CD}^H\mathbf{Q}\mathbf{h}_{CD}+\sigma^2} \ge \gamma_d\\ & \frac{\mathbf{h}_{BE}^H\mathbf{V}\mathbf{h}_{BE}}{\mathbf{h}_{CE}^H\mathbf{Q}\mathbf{h}_{CE}+\sigma^2} \le \gamma_e\\ & \mathbf{e}_i^T\mathbf{Q}\mathbf{e}_i \le P_i, i=1,2,\ldots,N\\ & \mathbf{V} \succeq \mathbf{0}, \mathbf{Q} \succeq \mathbf{0}\\ & \mathbf{V} = \mathbf{v}\mathbf{v}^H. \end{aligned} \tag{14}$$

Similar to last subsection, the constraint $\mathbf{V} = \mathbf{v}\mathbf{v}^H$ can be relaxed (proof is similar to the Appendix). Without this rank constraint, similar to last subsection, (14) can be rewritten as

$$\begin{aligned}\min_{\mathbf{V},\mathbf{Q}}\ & \mathrm{Tr}(\mathbf{V})\\ \text{s.t.}\ & \gamma_d\Big(\mathrm{Tr}(\mathbf{H}_{CD}\mathbf{Q}) + \sigma^2\Big) - \mathrm{Tr}(\mathbf{H}_{BD}\mathbf{V}) \le 0\\ & \mathrm{Tr}(\mathbf{H}_{BE}\mathbf{V}) - \gamma_e\Big(\mathrm{Tr}(\mathbf{H}_{CE}\mathbf{Q}) + \sigma^2\Big) \le 0\\ & \mathrm{Tr}\Big(\mathbf{e}_i\mathbf{e}_i^T\mathbf{Q}\Big) \le P_i, i=1,2,\ldots,N\\ & \mathbf{V} \succeq \mathbf{0}, \mathbf{Q} \succeq \mathbf{0}. \end{aligned} \tag{15}$$

Since (15) is a standard SDP problem, its optimal solution $(\mathbf{V}^*, \mathbf{Q}^*)$ can be found by using CVX tools. Moreover, $\mathbf{V}^*$ can be written as $\mathbf{v}^*\mathbf{v}^{*\mathbf{H}}$ through eigenvalue decomposition. Therefore (13) is solved and its optimal solution is $(\mathbf{v}^*, \mathbf{Q}^*)$.

C. Complexity Analysis

In the following, the complexity of the proposed schemes will be analyzed according to the result in [25]. The complexity derived in [25] is

$$\mathcal{O}\left(\left(1+\sum_{j=1}^{J}k_j\right)^{\frac{1}{2}}\left(n^3+n^2\sum_{j=1}^{J}k_j^2+n\sum_{j=1}^{J}k_j^3\right)\log\frac{1}{\epsilon}\right), \tag{16}$$

where ϵ represents a tolerable error, k_j, J and n denote the dimension of the j-th constraint, the number of constraints (one equality constraint equals two inequality ones) and the total dimension of all optimization variables, respectively.

As for B-CJ-SRM, according to (11), we have $J = N + 6$, $k_1 = k_2 = k_3 = \cdots = k_{N+4} = 1$, $k_{N+5} = M$, $k_{N+6} = N$, $n = M^2 + N^2 + 1$. In order to differentiate the same n for other schemes, here n is renamed as n_0. Then the complexity of B-CJ-SRM is

$$\begin{aligned}\mathcal{O}\Big(\sqrt{M+2N+5}\Big(&n_0^2 + n_0(M^2+N^2+N+4)\\ &+ M^3+N^3+N+4\Big)n_0\log\frac{1}{\epsilon}\Big). \end{aligned} \tag{17}$$

Similarly, for B-CJ-TPM, according to (15), we have $J = N + 4$, $k_1 = k_2 = k_3 = \cdots = k_{N+2} = 1$, $k_{N+3} = M$,

$k_{N+4} = N$, $n = n_1 = M^2 + N^2$. The complexity of B-CJ-TPM is calculated as

$$\mathcal{O}\Big(\sqrt{M+2N+3}\Big(n_1^2 + n_1(M^2+N^2+N+2) + M^3+N^3+N+2\Big)n_1 \log\frac{1}{\epsilon}\Big). \quad (18)$$

Given M, it can be derived from (17) and (18) that both the complexity of B-CJ-SRM and B-CJ-TPM is approximately $\mathcal{O}(N^{6.5})$. Due to this high complexity, alternative schemes will be investigated in the next section.

IV. Proposed Low-Complexity Schemes

Due to time-varying characteristic of wireless channel, the BS should solve the optimization problems quickly to renew the optimal $\mathbf{v}$ and $\mathbf{Q}$ in time. So the proposed schemes should not only obtain the best secrecy or power but also have low complexity. Different from B-CJ-SRM and B-CJ-TPM optimizing the matrix $\mathbf{V}$ that has quadratic dimensions, low complex schemes namely LC-B-CJ-SRM and LC-B-CJ-TPM proposed in this section will directly optimize $\mathbf{v}$ and obtain sub-optimal solutions. The main ideas of two low-complexity schemes are illustrated as follows. Firstly, if necessary, the optimization problem is transformed into an equivalent difference of convex (DC) programming [26]. Then the CCCP iterative algorithm is used to solve the DC programming.

A. Proposed LC-B-CJ-SRM

Since (8) is a nonconvex problem, we first transform it into an equivalent DC programming and then solve it by CCCP-based iterative algorithm. We first rewrite the interference signals transmitted by cooperative nodes as $\boldsymbol{q} \circ \mathbf{z}$, where $\circ$ represents Hadamard product, $\mathbf{z} = [z_1, z_2, \ldots, z_N]$ contains ANs generated by cooperative nodes, $\mathbf{q} = [q_1, q_2, \ldots, q_N]^T$ is a weight vector in which q_i denotes the weight for the ith cooperative node. Then we reformulate problem (8) as

$$\begin{aligned} \max_{\mathbf{v},\mathbf{q}} \ & \frac{\mathbf{v}^H\mathbf{A}\mathbf{v}}{\mathbf{q}^H\mathbf{B}\mathbf{q}+\sigma^2} \\ \text{s.t.} \ & \frac{\mathbf{v}^H\mathbf{C}\mathbf{v}}{\mathbf{q}^H\mathbf{D}\mathbf{q}+\sigma^2} \le \gamma_e \\ & \mathbf{v}^H\mathbf{v} \le P_{BS} \\ & {\mathbf{e}_i}^T\mathbf{q}\mathbf{q}^H\mathbf{e}_i \le P_i,\ i=1,2,\ldots,N, \end{aligned} \quad (19)$$

where $\mathbf{A} = \mathbf{h}_{BD}\mathbf{h}_{BD}^H$, $\mathbf{B} = \mathrm{diag}(|h_{C_1D}|^2, |h_{C_2D}|^2, \ldots, |h_{C_ND}|^2)$, $\mathbf{C} = \mathbf{h}_{BE}\mathbf{h}_{BE}^H$ and $\mathbf{D} = \mathrm{diag}(|h_{C_1E}|^2, |h_{C_2E}|^2, \ldots, |h_{C_NE}|^2)$. By introducing a slack variable t, we rewrite (19) as

$$\begin{aligned} \max_{\mathbf{v},\mathbf{q},t} \ & t \\ \text{s.t.} \ & \mathbf{q}^H\mathbf{B}\mathbf{q}+\sigma^2 - \frac{\mathbf{v}^H\mathbf{A}\mathbf{v}}{t} \le 0 \\ & \mathbf{v}^H\mathbf{C}\mathbf{v} - \gamma_e\Big(\mathbf{q}^H\mathbf{D}\mathbf{q}+\sigma^2\Big) \le 0 \\ & \mathbf{v}^H\mathbf{v} \le P_{BS} \\ & {\mathbf{e}_i}^T\mathbf{q}\mathbf{q}^H\mathbf{e}_i \le P_i,\ i=1,2,\ldots,N \\ & t > 0. \end{aligned} \quad (20)$$

Since t, $\mathbf{v}^H\mathbf{A}\mathbf{v}$ and $\mathbf{v}^H\mathbf{A}\mathbf{v}/t$ ($t > 0$, $\mathbf{A} \succeq 0$) are convex, (20) is a DC programming. In the following, CCCP-based iterative algorithm is used to find a local optimum of (20). Let

$$\zeta_{\mathbf{A}}(\mathbf{v}, t) = \frac{\mathbf{v}^H\mathbf{A}\mathbf{v}}{t}, \quad (21)$$

$$\psi_{\mathbf{A}}(\mathbf{v}) = \mathbf{v}^H\mathbf{A}\mathbf{v}. \quad (22)$$

According to [27], the first-order Tayor expansions of (21) and (22) around the point $(\tilde{\mathbf{v}}, \tilde{t})$ are computed as

$$\zeta_{\mathbf{A}}\big(\mathbf{v}, t, \tilde{\mathbf{v}}, \tilde{t}\big) = \frac{2\,\mathrm{Re}\{\tilde{\mathbf{v}}^H\mathbf{A}\mathbf{v}\}}{\tilde{t}} - \frac{\tilde{\mathbf{v}}^H\mathbf{A}\tilde{\mathbf{v}}}{\tilde{t}^2}t, \quad (23)$$

$$\psi_{\mathbf{A}}(\mathbf{v}, \tilde{\mathbf{v}}) = 2\,\mathrm{Re}\Big\{\tilde{\mathbf{v}}^H\mathbf{A}\mathbf{v}\Big\} - \tilde{\mathbf{v}}^H\mathbf{A}\tilde{\mathbf{v}}. \quad (24)$$

In the $(n+1)$th iteration of CCCP algorithm, we solve the following convex optimization problem.

$$\begin{aligned} \max_{\mathbf{v},\mathbf{q},t} \ & t && (25a) \\ \text{s.t.} \ & \mathbf{q}^H\mathbf{B}\mathbf{q}+\sigma^2 - \zeta_{\mathbf{A}}\Big(\mathbf{v}, t, \tilde{\mathbf{v}}^{(n)}, \tilde{t}^{(n)}\Big) \le 0 && (25b) \\ & \mathbf{v}^H\mathbf{C}\mathbf{v} - \gamma_e\Big(\psi_{\mathbf{D}}\Big(\mathbf{q}, \tilde{\mathbf{q}}^{(n)}\Big)+\sigma^2\Big) \le 0 && (25c) \\ & \mathbf{v}^H\mathbf{v} \le P_{BS} && (25d) \\ & {\mathbf{e}_i}^T\mathbf{q}\mathbf{q}^H\mathbf{e}_i \le P_i,\ i=1,2,\ldots,N. && (25e) \\ & t > 0. && (25f) \end{aligned}$$

where $(\tilde{\mathbf{v}}^{(n)}, \tilde{\mathbf{q}}^{(n)}, \tilde{t}^{(n)})$ is the solution at the nth iteration.

Equation (25) can be further transformed into a SOCP. Letting

$$\mathbf{a} = -\frac{2}{\tilde{t}^{(n)}}\mathbf{A}\tilde{\mathbf{v}}^{(n)}, \quad (26)$$

$$b = \frac{\Big(\tilde{\mathbf{v}}^{(n)}\Big)^H\mathbf{A}\tilde{\mathbf{v}}^{(n)}}{\Big(\tilde{t}^{(n)}\Big)^2}, \quad (27)$$

(25b) is rewritten as

$$\mathbf{q}^H\mathbf{B}\mathbf{q} + \mathrm{Re}\Big\{\mathbf{a}^H\mathbf{v}\Big\} + bt + \sigma^2 \le 0, \quad (28)$$

which is converted into a second-order cone (SOC) constraint

$$\left\|\begin{bmatrix} 2\mathbf{h}_{CD}^H\mathbf{q} \\ -\mathrm{Re}\Big\{\mathbf{a}^H\mathbf{v}\Big\} - bt - \sigma^2 - 1 \end{bmatrix}\right\| \le -\mathrm{Re}\Big\{\mathbf{a}^H\mathbf{v}\Big\} - bt - \sigma^2 + 1. \quad (29)$$

Similarly, (25c), (25d) and (25e) are also converted into SOC constraints. Thus (25) is converted into the following SOCP.

$$\begin{aligned} \max_{\mathbf{v},\mathbf{q},t} \ & t \\ \text{s.t.} \ & \left\|\begin{bmatrix} 2\mathbf{h}_{CD}^H\mathbf{q} \\ -\mathrm{Re}\Big\{\mathbf{a}^H\mathbf{v}\Big\} - bt - \sigma^2 - 1 \end{bmatrix}\right\| \le -\mathrm{Re}\Big\{\mathbf{a}^H\mathbf{v}\Big\} - bt - \sigma^2 + 1 \\ & \left\|\begin{bmatrix} 2\mathbf{h}_{BE}^H\mathbf{v} \\ -\mathrm{Re}\Big\{\mathbf{c}^H\mathbf{q}\Big\} - d + \sigma^2 - \gamma_e \end{bmatrix}\right\| \le -\mathrm{Re}\Big\{\mathbf{c}^H\mathbf{q}\Big\} - d + \sigma^2 + \gamma_e \\ & \|\mathbf{v}\| \le \sqrt{P_{BS}},\ \Big\|{\mathbf{e}_i}^T\mathbf{q}\Big\| \le \sqrt{P_i}, i=1,2,\ldots,N,\ t > 0, \end{aligned} \quad (30)$$

Algorithm 1 The Proposed LC-B-CJ-SRM Scheme

Initialization:
1) Given P_{BS}, P_i, γ_e, N, M, σ^2 and θ_1;
2) $n = 0$, $(\tilde{\mathbf{v}}^{(n)}, \tilde{\mathbf{q}}^{(n)}, \tilde{t}^{(n)}) = (\mathbf{v}_0, \mathbf{q}_0, t_0)$;
Repeat:
1) Solve (30) with $(\tilde{\mathbf{v}}^{(n)}, \tilde{\mathbf{q}}^{(n)}, \tilde{t}^{(n)})$ and obtain current optimal solution $(\mathbf{v}^*, \mathbf{q}^*, t^*)$;
2) Update $(\tilde{\mathbf{v}}^{(n+1)}, \tilde{\mathbf{q}}^{(n+1)}, \tilde{t}^{(n+1)})$=$(\mathbf{v}^*, \mathbf{q}^*, t^*)$, n=n+1;
3) Compute $|\tilde{t}^{(n+1)} - \tilde{t}^{(n)}|$;
Until: $|\tilde{t}^{(n+1)} - \tilde{t}^{(n)}| < \theta_1$;
Return: local optimal solution of (19): $(\mathbf{v}^*, \mathbf{q}^*)$.

where

$$\mathbf{c} = -2\mathbf{D}\tilde{\mathbf{q}}^{(n)}, \tag{31}$$

$$d = \left(\tilde{\mathbf{q}}^{(n)}\right)^H \mathbf{D}\tilde{\mathbf{q}}^{(n)}. \tag{32}$$

The above scheme is summarized as Algorithm 1.

B. Proposed LC-B-CJ-TPM

For the optimization problem (13), we first transform it into an equivalent DC programming

$$\min_{\mathbf{v},\mathbf{q}} \quad \|\mathbf{v}\|^2 \tag{33a}$$

$$\text{s.t.} \quad \mathbf{q}^H\mathbf{B}\mathbf{q} + \sigma^2 - \frac{1}{\gamma_d}\mathbf{v}^H\mathbf{A}\mathbf{v} \le 0 \tag{33b}$$

$$\mathbf{v}^H\mathbf{C}\mathbf{v} - \gamma_e\left(\mathbf{q}^H\mathbf{D}\mathbf{q} + \sigma^2\right) \le 0 \tag{33c}$$

$$\mathbf{e}_i{}^T\mathbf{q}\mathbf{q}^H\mathbf{e}_i \le P_i,\ i = 1, 2, \ldots, N. \tag{33d}$$

In the following, the CCCP-based iteration algorithm will be used to solve (33). According to (22) and (24), we solve the following optimization problem in the $(n+1)$th iteration.

$$\min_{\mathbf{v},\mathbf{q}} \ \|\mathbf{v}\|^2 \tag{34a}$$

$$\text{s.t.} \ \ \mathbf{q}^H\mathbf{B}\mathbf{q} + \sigma^2 - \frac{1}{\gamma_d}\psi_{\mathbf{A}}\left(\mathbf{v}, \tilde{\mathbf{v}}^{(n)}\right) \le 0 \tag{34b}$$

$$\mathbf{v}^H\mathbf{C}\mathbf{v} - \gamma_e\left(\psi_{\mathbf{D}}\left(\mathbf{q}, \tilde{\mathbf{q}}^{(n)}\right) + \sigma^2\right) \le 0 \tag{34c}$$

$$\mathbf{e}_i{}^T\mathbf{q}\mathbf{q}^H\mathbf{e}_i \le P_i,\ i = 1, 2, \ldots, N. \tag{34d}$$

Equation (34) is further converted to a SOCP. Since (34b) and (34c) can be written as SOC constraints, (34) is equivalent to

$$\begin{aligned}
&\min_{\mathbf{v},\mathbf{q}} \ \|\mathbf{v}\|^2 \\
&\text{s.t.} \ \left\|\begin{bmatrix} 2\mathbf{h}_{CD}^H\mathbf{q} \\ -\frac{1}{\gamma_d}\,\mathrm{Re}\left\{\mathbf{a}_1{}^H\mathbf{v}\right\} - b_1 - 1 \end{bmatrix}\right\| \le -\frac{\mathrm{Re}\left\{\mathbf{a}_1{}^H\mathbf{v}\right\}}{\gamma_d} - b_1 + 1 \\
&\left\|\begin{bmatrix} 2\mathbf{h}_{CE}^H\mathbf{v} \\ -\mathrm{Re}\left\{\mathbf{c}^H\mathbf{q}\right\} - d_1 - \gamma_e \end{bmatrix}\right\| \le -\mathrm{Re}\left\{\mathbf{c}^H\mathbf{q}\right\} - d_1 + \gamma_e \\
&\left\|\mathbf{e}_i{}^T\mathbf{q}\right\| \le \sqrt{P_i}, i = 1, 2, \ldots, N,
\end{aligned} \tag{35}$$

where

$$\mathbf{a}_1 = -2\mathbf{A}\tilde{\mathbf{v}}^{(n)}, \tag{36}$$

Algorithm 2 The Proposed LC-B-CJ-TPM Scheme

Initialization:
1) Given P_i, R_s^0, γ_e, N, M, σ^2 and θ_2;
2) $n = 0$, $(\tilde{\mathbf{v}}^{(n)}, \tilde{\mathbf{q}}^{(n)}) = (\mathbf{v}_0, \mathbf{q}_0)$;
Repeat:
1) Solve (35) with $(\tilde{\mathbf{v}}^{(n)}, \tilde{\mathbf{q}}^{(n)})$ and obtain current optimal solution $(\mathbf{v}^*, \mathbf{q}^*)$;
2) Update $(\tilde{\mathbf{v}}^{(n+1)}, \tilde{\mathbf{q}}^{(n+1)}) = (\mathbf{v}^*, \mathbf{q}^*)$, $n = n + 1$;
3) Compute $|10lg(\|\tilde{\mathbf{v}}^{(n+1)}\|^2) - 10lg(\|\tilde{\mathbf{v}}^{(n)}\|^2)|$;
Until: $|10lg(\|\tilde{\mathbf{v}}^{(n+1)}\|^2) - 10lg(\|\tilde{\mathbf{v}}^{(n)}\|^2)| < \theta_2$.
Return: local optimal solution of (33): $(\mathbf{v}^*, \mathbf{q}^*)$.

$$b_1 = \frac{1}{\gamma_d}\left(\tilde{\mathbf{v}}^{(n)}\right)^H\mathbf{A}\tilde{\mathbf{v}}^{(n)} + \sigma^2, \tag{37}$$

$$d_1 = \left(\tilde{\mathbf{q}}^{(n)}\right)^H\mathbf{D}\tilde{\mathbf{q}}^{(n)} - \sigma^2. \tag{38}$$

The LC-B-CJ-TPM scheme is summarized as Algorithm 2.

C. Complexity Analysis

Similar to the complexity analysis for B-CJ-SRM, the complexity of LC-B-CJ-SRM is calculated as follows. In (30), the number of LMI constraints is $J = N + 4$, each LMI has one dimension, i.e., $k_1 = k_2 = k_3 = \cdots = k_{N+4} = 1$, the total dimensions of all optimization variables $n = n_2 = M + N + 1$. According to (16), the complexity of LC-B-CJ-SRM is expressed as

$$\mathcal{O}\left(\sqrt{N+5}\left(n_2^2 + n_2(N+4) + N + 4\right)n_2 \log\frac{1}{\epsilon}\right) \cdot I_{max}, \tag{39}$$

where I_{max} is the maximum number of iteration times.

Similarly, for LC-B-CJ-TPM, according to its corresponding SOCP optimization problem (35), we have $J = N + 2$, $k_1 = k_2 = k_3 = \ldots = k_{N+2} = 1$, $n = n_3 = M + N$. The complexity of LC-B-CJ-TPM is calculated as

$$\mathcal{O}\left(\sqrt{N+2}\left(n_3^2 + n_2(N+2) + N + 2\right)n_3 \log\frac{1}{\epsilon}\right) \cdot I_{max}. \tag{40}$$

It can be derived from (39) and (40) that both the complexity of LC-B-CJ-SRM and LC-B-CJ-TPM is approximately $\mathcal{O}(N^{3.5})$, much lower than B-CJ-SRM and B-CJ-TPM.

V. Simulation and Discussion

In this section, we simulate and evaluate 6 wireless powered PHY security schemes, including our proposed two optimal schemes (B-CJ-SRM and B-CJ-TPM), proposed two low-complexity schemes (LC-B-CJ-SRM and LC-B-CJ-TPM), zero-forcing scheme [8] and QoSD scheme [18]. The performance of these schemes will be compared in terms of SR and the transmit power of the BS. In the simulations, one destination user and one eavesdropper locate in a city bus which moves in a low speed. Due to the slow move, the distance between the BS and the bus is nearly unchanged in a short duration. Logarithmic distance path loss model is employed,

TABLE I
SIMULATION PARAMETERS

Parameter	Value
pathloss factor between BS and user	3
pathloss factor between users	4
M (number of BS antennas)	4 to 48; default 8
N (number of jamming nodes)	2 to 30; default 4
P_{BS} (BS transmit power in dBm)	30 to 50; default 40
P_i (harvested power in mW)	1 to 10; default 2.5
σ^2 (noise variance)	10^{-8}
γ_e (eavesdropper's SINR threshold)	0.1
R_s^0 (minimum secrecy rate)	2 bits/s/Hz
γ_d (destination's SINR threshold)	3.4
θ_1 (LC-B-CJ-SRM converge threshold)	0.01
θ_2 (LC-B-CJ-TPM converge threshold)	1

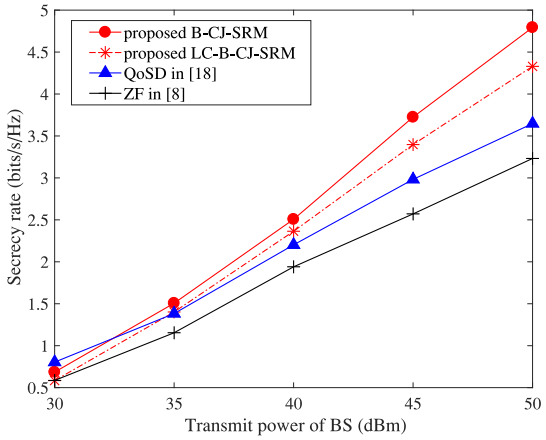

Fig. 2. Secrecy rate versus BS transmit power ($M = 8$, $N = 4$, $P_i = 2.5mW$).

where the attenuation factor n is assumed to be 3 for the transmission channel and wiretap channel. Inside the vehicle, n is assumed to be 4 [28], [29]. The channel between the BS and the destination user (or the eavesdropper) is assumed to follow Rayleigh distribution for the block of line-of-sight (LOS) components in urban areas, while the channel between nodes inside the bus follows Rice distribution for the LOS existence. The noise is assumed to follow a complex Gaussian distribution with mean 0 and variance 10^{-8}.

Fig. 2 shows how the SR changes with the transmit power of the BS. From this figure, we can observe that when the transmit power of the BS increases, the SR of each scheme also increases. The reason is explained as follows. According to (7), the SR is determined by the destination's SINR and the eavesdropper's SINR. As the BS increases its transmit power, both SINRs become larger. Meanwhile, the destination's SINR increases more than the eavesdropper's SINR because essentially the optimization problems of the aforementioned schemes all make efforts to limit the eavesdropper's SINR.

It can also be observed that our proposed low-complexity scheme has similar performance to B-CJ-SRM. Moreover, our B-CJ-SRM scheme always outperforms zero-forcing method and in the case of high transmit power (more than 36dBm) also

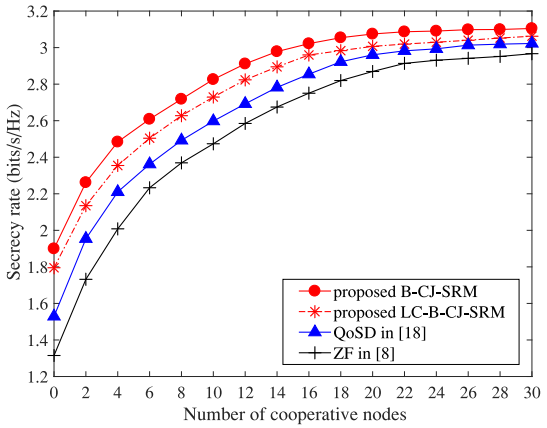

Fig. 3. Secrecy rate versus the number of cooperative nodes ($M = 8$, $P_i = 2.5mW$, $P_{BS} = 10W$).

outperforms QoSD method. The performance gap enlarges with the increase of transmit power. The reason is explained as follows. Our method is to obtain the maximum SINR of the destination, but zero-forcing and QoSD only force the interference to the destination to zero or set a minimum threshold for the destination's SINR. Although zero-forcing and QoSD aim to maximize the interference to the eavesdropper or to minimize the eavesdropper's SINR, the eavesdropper's SINR is so small that its reduction can be neglected. Therefore, our method has better SR than the other two methods and this advantage becomes wilder when the transmit power increases. When the transmit power of the BS is small (less than 36dBm), although our method has a slightly higher SR than zero-forcing, it performs worse than QoSD. The reason is that QoSD set a minimum required SINR for the destination which guarantees a relatively good SR in case of low transmit power.

Fig. 3 shows how the SR changes with the number of cooperative nodes. It can be observed that the secrecy in the case of 0 jammer is not so good as the case of at least 2 jammers. This phenomenon shows that jamming nodes can help to improve secrecy rate through interfering the eavesdropper.

When the number of jamming nodes increases, the secrecy rate also increases. The reason is explained as follows. With more cooperative nodes, more interference the eavesdropper will suffer, so the eavesdropper's SINR becomes smaller. Meanwhile, the destination's SINR experiences little degradation because the above schemes all have restrict requirement on the destination's SINR. As the eavesdropper's SINR decreases and the destination's SINR keeps relatively stable, the SR will increase with the number of cooperative nodes.

It can also be observed from Fig. 3 that the SRs of the four schemes become relatively steady when there are more than 24 cooperative nodes. The reason is explained as follows. With so many cooperative nodes, it is easy to generate great enough interference to the eavesdropper, forcing the eavesdropper's SINR to nearly 0. Meanwhile the dimension of interference covariance matrix is so high that it is easy to null out the interference to the destination, resulting in a stable SINR of the destination. As both SINRs of the destination and the eavesdropper are relatively steady, the SR will also keep stable.

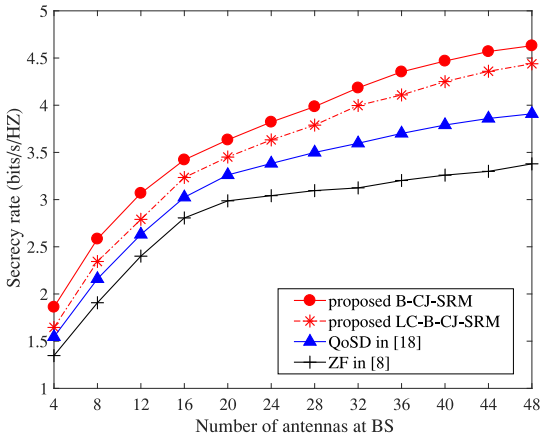

Fig. 4. Secrecy rate versus the number of antennas at the BS ($N = 4$, $P_i = 2.5mW$, $P_{BS} = 10W$).

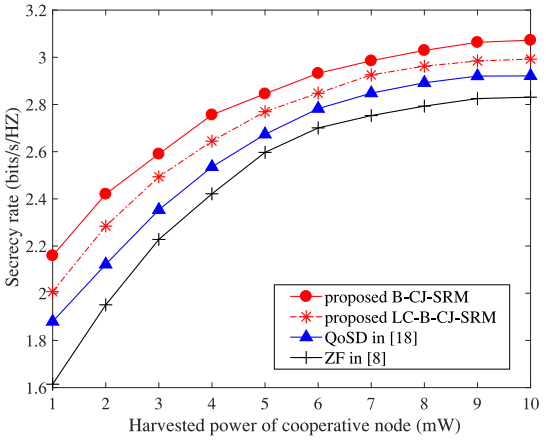

Fig. 5. Secrecy rate versus harvested power ($M = 8$, $N = 4$, $P_{BS} = 10W$).

Fig. 4 shows how the SR changes with the number of antennas at the BS. With more antennas at the BS, the SRs of our proposed two schemes increases. As the reason, with more antennas, the beamforming vector has a higher dimension, then it is easier for our schemes to maximize the desired user's SINR. In addition, the eavesdropper's SINR is always limited to a very low level. So the SR will increase. When the number of BS antennas and the number of cooperative nodes are both small (e.g., 4), with the limited dimension of $\mathbf{v}$ and $\mathbf{Q}$, both LC-B-CJ-SRM and QoSD cannot null out the interference at the destination. But zero-forcing scheme nulls it out through the corresponding constraint. So zero-forcing outperforms LC-B-CJ-SRM and QoSD in the case of few antennas.

Fig. 5 shows how the SR changes with the harvested power. All cooperative nodes are assumed to receive the same power. It is observed that with more harvested power, the SR gets better. The reason is as explained follows. Harvesting more energy, each cooperative node is able to transmit jamming signal in a higher power, increasing the interference to the eavesdropper. Meanwhile, the interference to the destination is limited to a very low level due to the optimization design of $\mathbf{Q}$. From all above analysis, it can be concluded that the SRs of the concerned schemes increase with the harvested power.

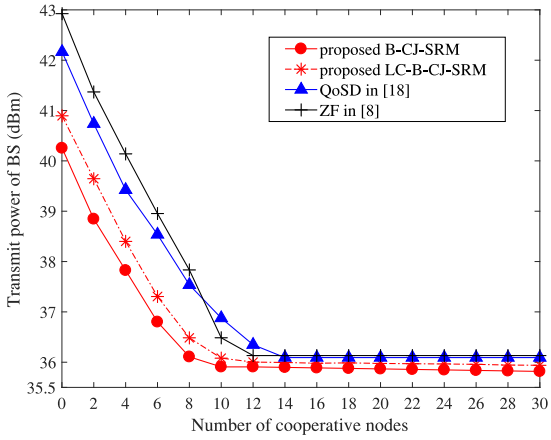

Fig. 6. Transmit power of the BS versus the number of cooperative nodes, where $M = 8$, $P_i = 2.5mW$, required minimum secrecy rate $R_S^0 = 2bits/s/Hz$.

From Fig. 5 it can also be observed that when the harvest power increases to more than 8mW, the SR grows slowly. The reason is that the relatively high transmit power of cooperative nodes will generate great interference to the eavesdropper, reducing its SINR to a very small value. Meanwhile the interference to the destination is very limited by designing the optimal $\mathbf{Q}$. So the SR will become relatively steady.

Fig. 6 shows how the transmit power of the BS changes with the number of cooperative nodes. It can be observed that under the same secrecy rate constraint, our proposed schemes require lower transmit power than other schemes. For example, when there are 8 jammers and the required minimum secrecy rate is 2 bits/s/Hz, the zero-forcing scheme requires the transmit power of the BS as high as 38.8 dBm (or 7.59 Watts), but our proposed B-CJ-TPM scheme requires a lower transmit power which is about 36.2 dBm (or 4.17 Watts).

In Fig. 6, the transmit power of the BS in the case of 0 jammer is higher than the case of at least 2 jammers, showing that CJ can help to reduce the transmit power through interfering the eavesdropper. It can also be observed that when there are more than 2 but less than 12 jamming nodes, the transmit power of the BS decreases as the number of jammers increases. The reason is explained as follows. The desired SR is achieved by the collaboration of the BS and the jammers. To bring forth the same SR, if the jammers make more contribution, the BS can contribute less. When there are more jammers, greater interference is generated to the eavesdropper, making a more positive impact on the desired SR. Then to keep the same SR, the BS has to reduce its transmit power.

It can also be observed from Fig. 6 that when the number of cooperative nodes is relatively large (e.g., greater than 12), the transmit power of the BS tends to be steady. The reason is that when there are enough jammers, considerable interference is generated to the eavesdropper, reducing the eavesdropper's SINR to nearly 0. Meanwhile, with a high dimension of the interference covariance matrix, the interference to the destination can be almost nulled out. So the SR will become relatively steady. In order to maintain the SR at 2 bits/s/Hz, the transmit power of the BS will be kept steady.

VI. Conclusion

This paper investigates wireless powered cooperative jamming to enhance energy-efficient security for public transportation. First, a CJ based secure communication model with energy harvesting is established. Both fixed and mobile jammers are employed to not only guarantee basic secrecy in the worst case but also endeavour to interfere with the eavesdropper. In addition, energy compensation is provided for mobile jammers through energy harvesting. Then to obtain the optimal performance, B-CJ-SRM and B-CJ-TPM schemes are proposed. These two schemes respectively maximize the SR and minimize the transmit power of the BS by the design of beamforming vector and interference covariance matrix. In order to further reduce the complexity, low-complexity versions namely LC-B-CJ-SRM and LC-B-CJ-TPM are proposed. Simulation results show that our proposed low-complexity schemes have similar performance to our optimal schemes. Moreover, when the transmit power of the BS is no less than 40dBm, our proposed schemes have significantly better performance than zero-forcing and QoSD methods. To achieve the same SR, when there are only a few jammers, our schemes requires less transmit power at the BS than other schemes.

Appendix

The optimization problem (11) is equivalent to

$$\begin{aligned}\min_{\tilde{\mathbf{V}},\tilde{\mathbf{Q}},t}\ & -\mathrm{Tr}\Big(\mathbf{H}_{BD}\tilde{\mathbf{V}}\Big)\\ \text{s.t.}\ & \mathrm{Tr}\Big(\tilde{\mathbf{V}}\Big)\le tP_{BS},\\ & \mathrm{Tr}\Big(\mathbf{e}_i\mathbf{e}_i^T\tilde{\mathbf{Q}}\Big)\le tP_i, i=1,2,\ldots,N,\\ & \mathrm{Tr}\Big(\mathbf{H}_{BE}\tilde{\mathbf{V}}\Big)-\gamma_e\Big(\mathrm{Tr}\Big(\mathbf{H}_{CE}\tilde{\mathbf{Q}}\Big)+\sigma^2 t\Big)\le 0,\\ & \mathrm{Tr}\Big(\mathbf{H}_{CD}\tilde{\mathbf{Q}}\Big)+\sigma^2 t=1,\\ & \tilde{\mathbf{V}}\succeq\mathbf{0},\quad \tilde{\mathbf{Q}}\succeq\mathbf{0},\end{aligned}\tag{41}$$

Since (41) satisfies Slater's constraint qualification [30], its objective function and constraints are all convex, and its optimal solution meets Karush-Kuhn-Tucker (KKT) conditions. The Lagrangian of (41) is

$$\begin{aligned}&\mathcal{L}\Big(\tilde{\mathbf{V}},\tilde{\mathbf{Q}},t,\lambda_1,\lambda_2,\lambda_3,\mu_i,\mathbf{P}_1,\mathbf{P}_2\Big)\\ &=-\mathrm{Tr}\Big(\mathbf{H}_{BD}\tilde{\mathbf{V}}\Big)+\lambda_1\Big(\mathrm{Tr}(\tilde{\mathbf{V}})-P_{BS}t\Big)\\ &\quad+\sum_{i=1}^{N}\mu_i\Big(\mathrm{Tr}\Big(\mathbf{e}_i\mathbf{e}_i^T\tilde{\mathbf{Q}}\Big)-P_it\Big)\\ &\quad+\lambda_2\Big(\mathrm{Tr}\Big(\mathbf{H}_{BE}\tilde{\mathbf{V}}\Big)-\gamma_e\Big(\mathrm{Tr}\Big(\mathbf{H}_{CE}\tilde{\mathbf{Q}}\Big)+\sigma^2t\Big)\Big)\\ &\quad+\lambda_3\Big(\mathrm{Tr}\Big(\mathbf{H}_{CD}\tilde{\mathbf{Q}}\Big)+\sigma^2t-1\Big)\\ &\quad-\mathrm{Tr}\Big(\mathbf{P}_1\tilde{\mathbf{V}}\Big)-\mathrm{Tr}\Big(\mathbf{P}_2\tilde{\mathbf{Q}}\Big).\end{aligned}\tag{42}$$

where $\lambda_1,\lambda_2,\lambda_3,\mathbf{P}_1,\mathbf{P}_2$ and μ_i are all dual variables associated with the constraints in (41). Let $\tilde{\mathbf{V}}^*$, $\tilde{\mathbf{Q}}^*$, t^* be the optimal primal variables and ${\lambda_1}^*$, ${\lambda_2}^*$, ${\lambda_3}^*$, ${\mathbf{P}_1}^*$, ${\mathbf{P}_2}^*$, ${\mu_i}^*$ be optimal dual variables, the KKT conditions that are relevant to the proof are listed as

$$\left.\frac{\partial L}{\partial\tilde{\mathbf{V}}}\right|_{\tilde{\mathbf{V}}=\tilde{\mathbf{V}}^*}=-\mathbf{H}_{BD}+{\lambda_1}^*\mathbf{I}+{\lambda_2}^*\mathbf{H}_{BE}-{\mathbf{P}_1}^*=\mathbf{0}\tag{43}$$

$${\mathbf{P}_1}^*\tilde{\mathbf{V}}^*=\mathbf{0}\tag{44}$$

$${\lambda_1}^*\Big(\mathrm{Tr}\Big(\tilde{\mathbf{V}}^*\Big)-P_{BS}t^*\Big)=0\tag{45}$$

$${\lambda_1}^*\ge 0,{\lambda_2}^*\ge 0\tag{46}$$

$${\mathbf{P}_1}^*\succeq\mathbf{0},\tilde{\mathbf{V}}^*\succeq\mathbf{0}\tag{47}$$

Let both sides of (43) be multiplied by $\tilde{\mathbf{V}}^*$ and substitute (44) into (43), we have

$$\mathbf{H}_{BD}\tilde{\mathbf{V}}^*=({\lambda_1}^*\mathbf{I}+{\lambda_2}^*\mathbf{H}_{BE})\tilde{\mathbf{V}}^*.\tag{48}$$

From (45), if ${\lambda_1}^*$ is 0, $\mathrm{Tr}(\tilde{\mathbf{V}}^*)-P_{BS}t^*$ can take any value, meaning that the transmit power $\mathrm{Tr}(\mathbf{V}^*)$ does not definitively equal the maximum value P_{BS}. Thus $\tilde{\mathbf{V}}^*$ in this condition is not the optimal solution, which is conflict with previous assumption. So ${\lambda_1}^*$ cannot be 0. Since ${\lambda_1}^*>0$, ${\lambda_1}^*\mathbf{I}+{\lambda_2}^*\mathbf{H}_{BE}$ in (48) is a positive definite matrix and also a full rank matrix. Then we perform rank operation on both sides of (48), i.e.,

$$\mathrm{rank}\Big(\mathbf{H}_{BD}\tilde{\mathbf{V}}^*\Big)=\mathrm{rank}\Big(\tilde{\mathbf{V}}^*\Big).\tag{49}$$

Exploiting rank(**AB**) $\le$ min{rank(**A**), rank(**B**)}, we have

$$\mathrm{rank}\Big(\tilde{\mathbf{V}}^*\Big)\le\min\Big\{\mathrm{rank}(\mathbf{H}_{BD}),\mathrm{rank}\Big(\tilde{\mathbf{V}}^*\Big)\Big\}.\tag{50}$$

Since $\mathrm{rank}(\mathbf{H}_{BD})=1$, $\mathrm{rank}(\tilde{\mathbf{V}}^*)\le 1$. Because $\mathbf{V}^*=\tilde{\mathbf{V}}^*/t^*$, we can conclude that $\mathrm{rank}(\mathbf{V}^*)\le 1$, and the proof is completed.

References

[1] F. Xiao, X. Xie, Z. Jiang, L. Sun, and R. Wang, "Utility-aware data transmission scheme for delay tolerant networks," *Peer-to-Peer Netw. Appl.*, vol. 9, no. 5, pp. 936–944, Sep. 2016.

[2] F. Shu, L. Xu, J. Wang, W. Zhu, and Z. Xiaobo, "Artificial-noise-aided secure multicast precoding for directional modulation systems," *IEEE Trans. Veh. Technol.*, vol. 67, no. 7, pp. 6658–6662, Jul. 2018.

[3] A. D. Wyner, "The wire-tap channel," *Bell Syst. Tech. J.*, vol. 54, no. 8, pp. 1355–1387, Oct. 1975.

[4] L. Zhang, H. Zhang, D. Wu, and D. Yuan, "Improving physical layer security for MISO systems via using artificial noise," in *Proc. Glob. Commun. Conf.*, Dec. 2015, pp. 1–6.

[5] F. Shu, X. Wu, J. Hu, R. Chen, J. Li, and J. Wang, "Secure and precise wireless transmission for random-subcarrier-selection-based directional modulation transmit antenna array," *IEEE J. Sel. Areas Commun.*, vol. 36, no. 4, pp. 890–904, Apr. 2018.

[6] F. Shu *et al.*, "Low-complexity and high-resolution DOA estimation for hybrid analog and digital massive MIMO receive array," *IEEE Trans. Commun.*, vol. 66, no. 6, pp. 2487–2501, Jun. 2018.

[7] E. Tekin and A. Yener, "The general Gaussian multiple-access and two-way wiretap channels: Achievable rates and cooperative jamming," *IEEE Trans. Inf. Theory*, vol. 54, no. 6, pp. 2735–2751, Jun. 2008.

[8] L. Dong, Z. Han, A. P. Petropulu, and H. V. Poor, "Improving wireless physical layer security via cooperating relays," *IEEE Trans. Signal Process.*, vol. 58, no. 3, pp. 1875–1888, Mar. 2010.

[9] S. Goel and R. Negi, "Guaranteeing secrecy using artificial noise," *IEEE Trans. Wireless Commun.*, vol. 7, no. 6, pp. 2180–2189, Jun. 2008.

[10] S. Bi, C. K. Ho, and R. Zhang, "Wireless powered communication: Opportunities and challenges," *IEEE Commun. Mag.*, vol. 53, no. 4, pp. 117–125, Apr. 2015.

[11] F. Xiao, X. Yang, M. Yang, L. Sun, R. Wang, and P. Yang, "Surface coverage algorithm in directional sensor networks for three-dimensional complex terrains," *Tsinghua Sci. Technol.*, vol. 21, no. 4, pp. 397–406, Aug. 2016.

[12] H. Ju and R. Zhang, "Optimal resource allocation in full-duplex wireless-powered communication network," *IEEE Trans. Commun.*, vol. 62, no. 10, pp. 3528–3540, Oct. 2014.
[13] H. Lee, S.-R. Lee, K.-J. Lee, H.-B. Kong, and I. Lee, "Optimal beamforming designs for wireless information and power transfer in MISO interference channels," *IEEE Trans. Wireless Commun.*, vol. 14, no. 9, pp. 4810–4821, Sep. 2015.
[14] L. Tang and Q. Li, "Wireless power transfer and cooperative jamming for secrecy throughput maximization," *IEEE Wireless Commun. Lett.*, vol. 5, no. 5, pp. 556–559, Oct. 2016.
[15] A. E. Shafie, A. Mabrouk, K. Tourki, N. Al-Dhahir, and R. Hamila, "Securing untrusted RF-EH relay networks using cooperative jamming signals," *IEEE Access*, vol. 5, pp. 24353–24367, 2017.
[16] G. Zhang, J. Xu, Q. Wu, M. Cui, X. Li, and F. Lin, "Wireless powered cooperative jamming for secure OFDM system," *IEEE Trans. Veh. Technol.*, vol. 67, no. 2, pp. 1331–1346, Feb. 2018.
[17] H. Chen, C. Zhai, Y. Li, and B. Vucetic, "Cooperative strategies for wireless-powered communications: An overview," *IEEE Wireless Commun.*, vol. 25, no. 4, pp. 112–119, Aug. 2018.
[18] H. Ma, J. Cheng, X. Wang, and P. Ma, "Robust MISO beamforming with cooperative jamming for secure transmission from perspectives of QoS and secrecy rate," *IEEE Trans. Commun.*, vol. 66, no. 2, pp. 767–780, Feb. 2018.
[19] K. Kwak, S. Lee, H. Min, S. Choi, and D. Hong, "New OFDM channel estimation with dual-ICI cancellation in highly mobile channel," *IEEE Trans. Wireless Commun.*, vol. 9, no. 10, pp. 3155–3165, Oct. 2010.
[20] H. Tang, Z. Ding, and B. C. Levy, "Enabling D2D communications through neighbor discovery in LTE cellular networks," *IEEE Trans. Signal Process.*, vol. 62, no. 19, pp. 5157–5170, Oct. 2014.
[21] X. Zhou *et al.*, "Secure SWIPT for directional modulation-aided AF relaying networks," *IEEE J. Sel. Areas Commun.*, vol. 37, no. 2, pp. 253–268, Feb. 2019.
[22] A. Charnes and W. W. Cooper, "Programming with linear fractional functionals," *Naval Res. Logistics Quart.*, vol. 9, nos. 3–4, pp. 181–186, 1962.
[23] L. Gui *et al.*, "DV-hop localization with protocol sequence based access," *IEEE Trans. Veh. Technol.*, vol. 67, no. 10, pp. 9972–9982, Oct. 2018.
[24] F. Xiao, Z. Wang, N. Ye, R. Wang, and X.-Y. Li, "One more tag enables fine-grained RFID localization and tracking," *IEEE/ACM Trans. Netw.*, vol. 26, no. 1, pp. 161–174, Feb. 2018.
[25] A. Ben-Tal and A. Nemirovski, *Lectures on Modern Convex Optimization: Analysis, Algorithms, and Engineering Applications*. Philadelphia, PA, USA: Soc. Ind. Appl. Math., 2001.
[26] R. Horst and N. V. Thoai, "DC programming: Overview," *J. Optim. Theory Appl.*, vol. 103, no. 1, pp. 1–43, Oct. 1999.
[27] E. Ziegel, "Matrix differential calculus with applications in statistics and econometrics," *Technometrics*, vol. 31, no. 4, pp. 501–502, Feb. 1989.
[28] P. Handayani, L. Mubarokah, and G. Hendrantoro, "Pathloss and shadowing characteristics in indoor environment at 2.4 GHz band," in *Proc. Int. Seminar Intell. Technol. Appl. (ISITIA)*, May 2015, pp. 423–428.
[29] L. Gui, M. Yang, H. Yu, J. Li, F. Shu, and F. Xiao, "A Cramer–Rao lower bound of CSI-based indoor localization," *IEEE Trans. Veh. Technol.*, vol. 67, no. 3, pp. 2814–2818, Mar. 2018.
[30] S. P. Boyd and L. Vandenberghe, *Convex Optimization*. Cambridge, U.K.: Cambridge Univ. Press, Mar. 2004.

Linqing Gui received the master's degree in electronic engineering from Shanghai Jiao Tong University, Shanghai, China, in 2009 and the Ph.D. degree in information science from INSA-Toulouse, Toulouse, France, in 2013. He is currently an Associate Professor with the School of Electronic and Optical Engineering, Nanjing University of Science and Technology, Nanjing, China. His main research interests are wireless communication and Internet of Things.

Bo He received the B.S. degree from Hefei University, Anhui, China, in 2016. He is currently pursuing the M.S. degree with the School of Electronic and Optical Engineering, Nanjing University of Science and Technology. His main research interests are wireless communication and Internet of Things.

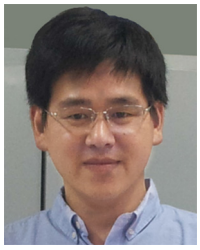

Xiaobo Zhou received the M.S. degree from the School of Electronic Science and Engineering, Anhui University, China, in 2010. He is currently pursuing the Ph.D. degree with the School of Electronic and Optical Engineering, Nanjing University of Science and Technology. Since 2010, he has been a Teacher with the School of Physics and Electronic Engineering, Fuyang Normal University. His main research interests are physical layer security, covert communications, and UAV communications.

Chunhua Yu received the B.E. degree in electrical engineering from the Harbin Institute of Technology, Harbin, China, in 1999, the M.S. degree in radio engineering from Southeast University, Nanjing, China, in 2004, and the Ph.D. degree in electronic science and engineering from Nanjing University, Nanjing, in 2015. He is currently with Nanjing University. His research interests include array signal processing and radar signal processing.

Feng Shu received the B.S. degree from Fuyang Normal University, Fuyang, China, in 1994, the M.S. degree from Xidian University, Xi'an, China, in 1997, and the Ph.D. degree from Southeast University, Nanjing, China, in 2002. From October 2003 to October 2005, he was a Post-Doctoral Researcher with the National Key Mobile Communication Laboratory, Southeast University. From September 2009 to September 2010, he was a Visiting Post-Doctoral Fellow with the University of Texas at Dallas. In October 2005, he joined the School of Electronic and Optical Engineering, Nanjing University of Science and Technology, Nanjing, where he is currently a Professor and a Supervisor of Ph.D. and graduate students. He is also with Fujian Agriculture and Forestry University and awarded with Mingjian Scholar Chair Professor in Fujian Province. His research interests include wireless networks, wireless location, and array signal processing. He has published about 200 papers, of which over 100 are in archival journals, including over 40 papers on IEEE Journals and 70 SCI-indexed papers. He holds six Chinese patents. He serves as an Editor for the IEEE ACCESS.

Jun Li (SM'16) received the Ph.D. degree in electronic engineering from Shanghai Jiao Tong University, Shanghai, China, in 2009. From January 2009 to June 2009, he was with the Department of Research and Innovation, Alcatel Lucent Shanghai Bell as a Research Scientist. From June 2009 to April 2012, he was a Post-Doctoral Fellow with the School of Electrical Engineering and Telecommunications, University of New South Wales, Australia. From April 2012 to June 2015, he was a Research Fellow with the School of Electrical Engineering, University of Sydney, Australia. Since 2015, he has been a Professor with the Nanjing University of Science and Technology, Nanjing, China. His research interests include network information theory, ultradense wireless networks, and mobile edge computing.